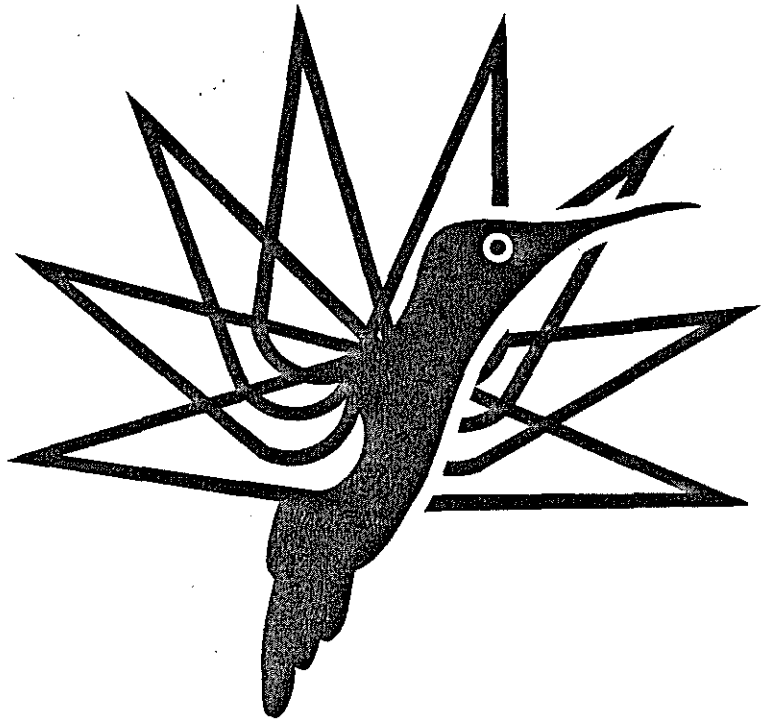

HIGHER ORDER PANEL METHOD
APPLIED TO VORTICITY-TRANSPORT-EQUATION

by
Wolfgang Send

Institut für Aeroelastik der DFVLR
D - 3400 Göttingen, Bunsenstrasse 10

FIFTH EUROPEAN ROTORCRAFT AND POWERED LIFT AIRCRAFT FORUM
SEPTEMBER 4 – 7TH 1979 - AMSTERDAM, THE NETHERLANDS

HIGHER ORDER PANEL METHOD APPLIED TO VORTICITY-TRANSPORT-EQUATION

by
Wolfgang Send

Institut fuer Aeroelastik der DFVLR
D-3400 Goettingen, Bunsenstrasse 10

SUMMARY

Incompressible flow is governed by the vorticity-transport-equation, in which the viscous term goes to zero in the limiting case of very large Reynolds number. For aerodynamic configurations this particular case allows a physically meaningful solution by an infinitely thin boundary layer. The layer forms a two-dimensional domain of nonzero vorticity, in which panel methods are applied. The vector components vary linearly in both coordinates of each surface element and thus lead to a continuous two-dimensional vorticity field.
The method, in general, follows the ideas of PRAGER |1| and MARTENSEN |2|, where thickness and lift are exclusively produced by vorticity. The final solution is achieved by fulfilling the boundary condition, which requires zero relative velocity inside the moving body or wing. This turns out to be an intrinsic measure for the accuracy of a solution. Though the method is primarily designed to calculate unsteady airloads on rotor blades, firstly well known two-dimensional solutions of steady and unsteady cases are compared to three-dimensional computations for large aspect ratios.

1. Introduction

The conservation laws for mass and momentum of a fluid under isentropic conditions yield a system of differential equations for the velocity $\vec{v}(\vec{r},t)$ and the pressure $p(\vec{r},t)$:

$$\frac{1}{c_s^2}\frac{dp}{dt} = -\rho(p)\cdot \operatorname{div}\vec{v} \quad , \tag{1}$$

$$\rho(p)\frac{d\vec{v}}{dt} = -\operatorname{grad} p + \eta\,\Delta\vec{v} + \left(\zeta + \frac{\eta}{3}\right)\operatorname{grad}\operatorname{div}\vec{v} \quad . \tag{2}$$

The density $\rho(p)$ is a unique function of p and $c_s^2 = (dp/d\rho)_s$ the local speed of sound; η and ζ imply viscous effects. Equations (1) and (2) describe the behaviour of small disturbances in a compressible, viscous fluid.
A fundamental property of any vector field $\vec{v}$ is that it may be decomposed (under certain weak constraints) into the gradient of a scalar potential Φ, the curl of a divergence free vector potential $\vec{A}$ and constant $\vec{v}_\infty$, where $\vec{v}$ has to converge uniformly against $\vec{v}_\infty$ at infinity (e.g. |3|, p.97):

$$\vec{v} = \vec{v}_\infty - \operatorname{grad}\Phi + \operatorname{rot}\vec{A} \quad , \quad \operatorname{div}\vec{A} = 0 \quad . \tag{3}$$

Since the fluid is assumed to be at rest for sufficiently large distances from the body, $\vec{v}_\infty$ is identically zero in the following treatment. The two classical approximations of (1) and (2) in aerodynamics coincide with the mathematical simplification, to use either Φ or $\vec{A}$ for a description of the velocity field. This is compressible, inviscid flow, on the one hand, and incompressible, viscous flow, on the other hand. Introducing curl and divergence of $\vec{v}$:

$$\delta = \operatorname{div} \vec{v} \ , \qquad \vec{j} = \operatorname{rot} \vec{v} \tag{4}$$

equation (3) results into two Poisson equations for the "source" terms δ and $\vec{j}$:

$$-\delta = \Delta\Phi \ , \qquad -\vec{j} = \Delta\vec{A} \ . \tag{5}$$

(4.2) implies $\operatorname{div} \vec{j} = 0$, which is the differential formulation of the conservation law for vorticity. Vanishing viscosity allows a first integral of (2) called Bernoulli's equation:

$$\int_{p_\infty}^{p} \frac{dp'}{\rho(p')} = \frac{d\Phi}{dt} + \frac{1}{2} \vec{v}^{\,2} \ . \tag{6}$$

Differentiating both sides with respect to time gives the well known equation for compressible flow:

$$\frac{1}{c_s^2} \frac{d}{dt} \left[\frac{d\Phi}{dt} + \frac{1}{2} \vec{v}^{\,2} \right] - \Delta\Phi = 0 \ . \tag{7}$$

Infinite speed of sound is equivalent to zero divergence δ. Thus, computing the curl of (2) for this case leads to the vorticity-transport-equation:

$$\boxed{\frac{d\vec{j}}{dt} = \vec{j} \cdot \operatorname{grad} \vec{v} + \nu \Delta \vec{j}} \qquad \nu = \frac{\eta}{\rho_0} \ . \tag{8}$$

Equations (7) and (8) are highly nonlinear, and there exist no solutions obtained without further drastic approximations. The substantial derivative d/dt plays a major role in these equations. It discribes the variation of an infinitely small fluid element with respect to time:

$$\frac{d}{dt} = \frac{\partial}{\partial t} + \vec{v}_{rel} \operatorname{grad} \ . \tag{9}$$

$\vec{v}_{rel}$ is the relative velocity field of the particles in a fluid with respect to an arbitrarily accelerated coordinate system.

We assume that the aerodynamic configuration considered here is a rigid body, which performs pure kinematic motion without internal vibrations. The motion of the fluid as it is seen by an observer at rest arises only from the bodies displacement and goes to zero for sufficiently large distances from the body. In this space fixed coordinate system the relative velocity would be equal to the "induced" velocity $\vec{v}$.
The coordinate system adapted here is a body fixed one and $\vec{v}_{rel}$ also contains the apparent kinematic motion $\vec{v}_{kin}$ of the fluid:

$$\vec{v}_{rel}(\vec{r},t) = \vec{v}(\vec{r},t) - \vec{v}_{kin}(\vec{r},t) \quad . \tag{10}$$

$\vec{v}_{kin}$ consists of two parts; the translatory motion of the origin and the rotational part of the spinning or oscillating axes.

2. Vorticity-Transport-Equation (VTE)

The VTE (8) describes the process of transportion and diffusion of vorticity in a fluid. Vorticity arises from the boundary condition for viscous fluids, which requires zero relative velocity on the surface S of a moving body:

$$\vec{v}_{rel}(\vec{r},t) = 0 \qquad \forall\ \vec{r} \in S \quad . \tag{11}$$

An extensive discussion concerning the creation of vorticity is given by LIGHTHILL [4]. Therefore, approximations to the basic equations may be made principally in three different ways; by approximating

= the transport mechanism $\quad \frac{d}{dt}\vec{j} - \vec{j}\ \mathrm{grad}\vec{v}$, (12.1)

= the diffusion term $\quad \nu \Delta\vec{j}$, (12.2)

= the boundary condition $\quad$ Eq. (11) . (12.3)

All three types of approximation are frequently used in combination. We start with a discussion of equation (12.1). It should be mentioned, that the differential equation for the relative position vector $\delta\vec{r}$ between two neighbouring particles in a fluid is identically the same equation. It reads:

$$\frac{d}{dt}\delta\vec{r} = \delta\vec{r} \cdot \mathrm{grad}\vec{v} \tag{13}$$

and its meaning is obvious. Equation (12.1) set to zero and the meaning of (13) transferred to vorticity gives an immediate clue as to how vorticity is preserved. The vorticity, once loaded on an infinitely small fluid element, remains there unaltered except that its direction points always to one, and to the same neighbouring particle to which it pointed at the beginning of

the motion or loading. It thereby changes its orientation with respect to space. Taking the term $\nu \cdot \Delta\vec{j}$ into account means that vorticity is spread out around the original fluid element, but does not become lost. If the body considered now moves with a high average velocity u_∞, e.g. in negative x-direction:

$$\vec{v}_{kin} = \begin{bmatrix} -u_\infty \\ 0 \\ 0 \end{bmatrix} + \text{small time-dependent terms} \qquad (14)$$

and L is a typical length of the body, then the Reynolds number

$$Re = \frac{u_\infty \cdot L}{\nu} \qquad (15)$$

is also very high. Vorticity is washed down rapidly and diffusion takes place far away from the body where vorticity has been created. The term $1/Re * \Delta\vec{j}$ may be omitted under these circumstances, since it has no influence on the velocity around the body. In the limiting case of very high Reynolds number, the VTE remains as:

$$\frac{d}{dt}\vec{j} - \vec{j} \cdot \text{grad}\vec{v} = 0 \quad . \qquad (16)$$

This, of course, does by no means indicate that there is no viscosity, rather it is confined to an infinitely thin boundary layer.
The next simplification affects the change of orientation with respect to space. The term $\vec{j} * \text{grad}\vec{v}$ produces this effect. For sufficiently thin and suitably formed (streamlined) obstacles, the destortion of the wake produces only negligible effects and the interaction of vorticity on itself plays a minor role. In certain cases, however, these effects may become important and Eq. (16) may have to be completely solved; nevertheless, the term will be omitted here. At this state of approximation, equation (8) has considerably grown thinner and reads:

$$\frac{d}{dt}\vec{j} = 0 \quad . \qquad (17)$$

If we now assume that the induced velocity is small compared to the kinematic velocity, and we neglect the small time-dependent terms of $\vec{v}_{rel}$, then the differential equation finely reads:

$$\left(\frac{\partial}{\partial t} + u_\infty \frac{\partial}{\partial x}\right)\vec{j} = 0 \qquad (18)$$

and has the general solution:

$$\boxed{\vec{j}(\vec{r},t) = \vec{j}(u_\infty t - x, y, z)} \qquad (19)$$

This is the most simple description of a wake which is possible.

3. Boundary Conditions and Integral Equation

For simplicity, we will from now on consider the moving body to be a cylindrical surface S (airfoil), constituted by:

$$S = \left\{ \vec{r}(s,y) \,\middle|\, s \in [-1,+1],\ y \in [0,\Lambda] \right\} ; \quad x = \mathrm{sign}(s) \cdot s \tag{20}$$

where a negative sign of s describes the lower side of the airfoil and Λ is the aspect ratio. The infinitely thin boundary layer B for homogeneous onset flow coincides with S and, in addition, contains the wake domain (Fig. 1):

$$B = \left\{ \vec{r}(s,y) \,\middle|\, s \in (-\infty,+\infty),\ y \in [0,\Lambda] \right\} . \tag{21}$$

If the airfoil was set into motion a finite time ago, then the interval for s is also finite. Since B is uniquely defined by $\vec{r}(s,y)$, there exists in each point $p \in B$ a tangent space with an orthonormal basis $\{\vec{t}_s, \vec{t}_y, \vec{n}\}$, where

$$\vec{t}_s = \frac{\partial \vec{r}}{\partial s} \cdot \left| \frac{\partial \vec{r}}{\partial s} \right|^{-1}, \quad \vec{t}_y = \frac{\partial \vec{r}}{\partial y} \cdot \left| \frac{\partial \vec{r}}{\partial y} \right|^{-1}, \quad \vec{n} = \vec{t}_s \times \vec{t}_y . \tag{22}$$

The vorticity vector $\vec{j}$ is nonzero only on B and may be written:

$$\vec{j}(\vec{r},t) = j_s(s,y,t) \cdot \vec{t}_s(s,y) + j_y(s,y,t) \cdot \vec{t}_y(s,y) . \tag{23}$$

This is the simplification of prescribed wake geometry. Due to equation (5.2), $\vec{j}$ induces a velocity field:

$$\vec{v}^{\pm}(\vec{r},t) = \frac{1}{4\pi} \iint_{B^*} \left\{ j'_s \cdot \mathrm{grad}\left(\frac{1}{r}\right) \times \vec{t}'_s + j'_y \cdot \mathrm{grad}\left(\frac{1}{r}\right) \times \vec{t}'_y \right\} dB' \mp \frac{1}{2} \left\{ j_s \vec{t}_y - j_s \vec{t}_s \right\} \tag{24}$$

where the variables referred to by a prime are integrated.

$$r := \left| \vec{r} - \vec{r}' \right| , \quad B^* = \begin{cases} B - \{\vec{r}\} & \forall\ \vec{r} \in B \\ B & \forall\ \vec{r} \notin B \end{cases} . \tag{25}$$

The second term of the sum (24) makes sense only for $\vec{r} \in B$ and vanishes elsewhere. Plus and minus signs give the velocity on B, if $\vec{r}$ approaches a point on B along the positive or negative normal direction in p. The boundary condition (11) requires zero relative velocity on the surface, as well as inside the moving body. With respect to B, this is also the interior of B.

For any point $p \in S$ the equation

$$\vec{v}^{\pm}_{rel}(\vec{r},t) = \vec{v}^{\pm}(\vec{r},t) - \vec{v}_{kin}(\vec{r},t) \tag{26}$$

holds with the condition:

$$\boxed{\vec{v}^{-}_{rel}(\vec{r},t) \equiv 0} \quad . \tag{27}$$

This is explicitly:

$$\vec{v}^{-}_{rel} \cdot \vec{t}_s = 0 \quad , \tag{27.1}$$

$$\vec{v}^{-}_{rel} \cdot \vec{t}_y = 0 \quad , \tag{27.2}$$

$$\vec{v}^{-}_{rel} \cdot \vec{n} = 0 \quad . \tag{27.3}$$

If equations (27.1-.3) are fulfilled on B, then analytical continuation leads to (27) for the whole interior of S. Because Eq. (24) contains no discontinuity in normal direction, it also leads to the equation:

$$\boxed{\vec{v}^{+}_{rel} \cdot \vec{n} = 0} \quad . \tag{28}$$

The last equation is equivalent to (27.1-.2). Both formulations may be used to calculate the vorticity. They lead to fredholm integral equations of first or second kind. A more detailed discussion of the mathematical questions is given by KRESS [5]. Taking Eq. (28), for convenience sake, leads to the formulation which is explicitly solved:

$$\frac{1}{4\pi} \iint_B \left\{ j'_s \cdot \vec{n} \cdot \nabla\left(\frac{1}{r}\right) \times \vec{t}'_s + j'_y \cdot \vec{n} \cdot \nabla\left(\frac{1}{r}\right) \times \vec{t}'_y \right\} dB' = \vec{n} \cdot \vec{v}_{kin} \qquad \forall\ \vec{r} \in S \quad . \tag{29}$$

The domains of B and S have already been given in (20) and (21). It should be noted, that S is a subset of B. This reflects the fact that the total vorticity is known as soon as it has left the aerea S of production, i.e., the trailing edge in the approximation considered. This procedure avoids the splitting into free and bound vorticity.
The two components j_s and j_y are not independent, because $\vec{j}$ has to obey the conservation law $\operatorname{div} \vec{j} = 0$.

4. Solution and Applications

The "ansatz":

$$\vec{j}(\vec{r},t) = \operatorname{grad} \sigma(\vec{r},t) \times \vec{n}(\vec{r},t) \tag{30}$$

satisfies div $\vec{j} = 0$ by definition of $\vec{n}$. $\sigma(\vec{r},t)$ is a scalar function definded on B and has to be at least twice differentiable, where the second derivative remains continuous in the whole domain B. The reader, who is familiar with scalar potential formulations, should note, that these relations have not been explicitly taken into account until now. Besides having to fulfill this basic requirement, $\vec{j}$ has to fulfill an additional condition, which sometimes arises from the improper description of the profiles contour, or from the thin plate approximation. B is not completely closed, rather it has its own boundary ∂B. The condition is, that the component of $\vec{j}$ perpendicular to the boundary ∂B has to vanish on the boundary. Otherwise there would be sinks and sources of vorticity along ∂B and this, of course, is in conflict with the assumption that vorticity arises only from the integral equation as "generator". Let $\vec{N}$ be the inward unit normal of ∂B, then the additional condition reads:

$$\vec{j}(\vec{r},t) \cdot \vec{N}(\vec{r},t) = 0 \qquad \forall\, \vec{r} \in \partial B \quad . \tag{31}$$

If B is closed, Eq. (31) becomes superfluous, since there is not any longer a boundary ∂B present.
An important part of the integral equation is the wake domain, which equation (19) coarsely discribes. Together with the ansatz for $\vec{j}$ this equation gives:

$$\vec{j}(s,y,t) = \vec{j}(u_\infty t - s, y) = \begin{bmatrix} \dfrac{\partial}{\partial y} \\ -\dfrac{\partial}{\partial s} \end{bmatrix} \sigma(u_\infty t - s, y) \quad . \tag{32}$$

We assume now (again as the most simple case) steady flow with respect to the moving airfoil or a harmonic variation of $\vec{j}$ due to an oscillation of the wing, which has not to be defined here:

$$\vec{j}(s,y,t) = \vec{j}_0(y)\, e^{i(\omega t - ks)}, \qquad k := \frac{\omega}{u_\infty} \quad . \tag{33}$$

(33) compared to (32) gives for $\vec{j}_0(y)$:

$$\vec{j}_0(y) = \begin{bmatrix} \dfrac{\partial}{\partial y} \\ ik \end{bmatrix} \sigma_0(y) \quad . \tag{34}$$

The limiting case k -> 0 leads to $j_y = 0$ and is in agreement with the well known fact that for the steady case the vorticity perpendicular to the onset flow vanishes in the wake, in which the parallel component depends only on y.

This, however, must not lead to the conclusion that j_y vanishes necessarily for any steady case. The steady solution of (18) only requires:

$$\frac{\partial}{\partial s}\begin{bmatrix} j_s(s,y) \\ j_y(s,y) \end{bmatrix} = 0 \quad . \tag{35}$$

Whereas the first equation is fulfilled by $j_s(y)$ independent of s, the second equation is a boundary condition for j_y in the steady case at the trailing edge. It may be satisfied by $j_y = 0$, as is done in the thin plate approximation. The second possibility is to consider this equation as supplementary condition for the vorticity washed down from upper and lower side. This procedure leads to an excellent agreement between three-dimensional computions for large aspect ratios and the analytic solution of Jukowsky-profiles. Furthermore, the stagnation point at the trailing edge, due to the condition $j_y = 0$, is avoided. The stagnation point occurs in two-dimensional analytical solutions except in the Jukowsky-profile, which has a vanishing first derivative at the rear end of the contour. The occurence of such a stagnation point is equivalent to zero relative velocity. It may be avoided also in the theory of conformal mapping as KRAEMER [9] has shown by applying a condition, which forces the pressure to be constant at the trailing edge.
Based on the approximations given above there is no mathematical reason to have a stagnation point in three dimensions. It seems that this is also in agreement with the physical model. The vorticity sheet approximates the boundary layer. The relative velocity outside this layer should have a well defined value at the trailing edge, which is far from being zero.
Furthermore, these velocities should slightly differ for nonzero angles of attack. Mathematically this effect leads to a tangential discontinuity between the relative velocities of the particles coming from upper and lower side of the airfoil. In addition, these particles transport different amounts of vorticity due to their different history along the profile. In reality, this tangential discontinuity is completely unstable and results in a more or less extended domain of turbulent fluid, i.e., the wake in second order approximation, which exceeds the quite simple form of (19).

To solve the integral equation (29), the domain B is divided into small surface elements (panels); the downwash of upper and lower side is formed by half infinite strips (Fig. 2). If we denote the number of elements in s-direction by m, m=1(1)M, and in y-direction by n, n=1(1)N, then the function σ in each element (m,n) is a fourth order function with respect to the local panel coordinates ξ and η :

$$\sigma_{m,n}(\xi,\eta) = \sum_{\mu=1}^{3}\sum_{\nu=1}^{3} g_\mu(\xi)\, g_\nu(\eta)\, S_{\mu\nu}(m,n)\cdot e^{i\omega t} \quad . \tag{36}$$

Where:

$$\xi = \frac{s - s_m}{s_{m+1} - s_m}\,, \quad \eta = \frac{y - y_n}{y_{n+1} - y_n}\,; \qquad \begin{matrix}(s_1, y_1) & = (-1, 0)\\ \ldots \text{ etc.} & \\ (s_{M+1}, y_{N+1}) & = (1, \Lambda)\end{matrix} \quad . \tag{37}$$

The functions q_l, l=1(1)3, are defined as:

$$g_1 : \quad z \rightarrow 2\cdot(1-z)\cdot\left(\frac{1}{2} - z\right) \quad , \tag{38.1}$$

$$g_2 : \quad z \rightarrow 4\cdot z\cdot(1-z) \quad , \tag{38.2}$$

$$g_3 : \quad z \rightarrow 2\cdot z\cdot\left(z - \frac{1}{2}\right) \quad . \tag{38.3}$$

When defined in that way, they give for ξ and η equal 0.0, 0.5 or 1 just the values $S_{\mu\nu}$ for $\sigma(\xi,\eta)$, as shown in Fig. 3a and 3b. The quadratic variation of σ in both coordinates of each panel garantees at least a linear variation of $\vec{j}$ in both directions. Continuity of σ is easily achieved by overlapping the values of σ at the borderlines of each panel. The most labourious part is the continuity of $\vec{j}$ in both coordinates (s,y) on the domain B. The corresponding equations are omitted here because they would occupy too much space. The final result is a continuous vector function $\vec{j}(s,y)$ on B, in the sense that $\vec{j}$ varies linearly in each element with respect to s and y. Its value agrees with the values of $\vec{j}$ in the neighbouring panels. The second order terms, which mutually occur in j_s and j_y by definition of σ, are left as they are. They are indeed very small compared to the linear terms in all examples calculated. Continuity of σ and $\vec{j}$ together with the boundary conditions for $\vec{j}$, as they have been discussed, lead to the final result that the integral-equation (29) forms a system of linear equations for the unknown central coefficients $S_{22}(m,n)$. All coefficients $S_{\mu\nu}(k,l)$ with $\mu \neq \nu$ depend on all central coefficients $S_{22}(m,n)$. Their contribution to the integral equation has to be calculated with respect to each coefficient $S_{22}(m,n)$.
For the vorticity vector $\vec{j}$ we have in each element:

$$\vec{j}_{m,n}(s,y,t) = \begin{bmatrix} \dfrac{1}{y_{n+1} - y_n} \displaystyle\sum_{\mu=1}^{3}\sum_{\nu=1}^{3} g_\mu(\xi)\,\dot{g}_\nu(\eta)\,S_{\mu\nu}(m,n) \\ \dfrac{-1}{s_{m+1} - s_m} \displaystyle\sum_{\mu=1}^{3}\sum_{\nu=1}^{3} \dot{g}_\mu(\xi)\,g_\nu(\eta)\,S_{\mu\nu}(m,n) \end{bmatrix} \cdot e^{i\omega t} \tag{39}$$

where the components are given in each panel with respect to the tangent space introduced in equation (22). The dot means the first derivative of q_l in equation (38) with respect to the given argument ξ or η.

Equation (34) now reads for one half-infinite strip:

$$\vec{j}_{\varkappa,n}(s,y,t) = \begin{bmatrix} \dfrac{1}{y_{n+1} - y_n} & \displaystyle\sum_{\nu=1}^{3} \dot{g}_\nu(\eta)\, S_{\lambda\nu}(\varkappa,n) \\ ik & \displaystyle\sum_{\nu=1}^{3} g_\nu(\eta)\, S_{\lambda\nu}(\varkappa,n) \end{bmatrix} \cdot e^{i(\omega t - ks)} \qquad (40)$$

upper side: $\varkappa = M,\ \lambda = 3$;

lower side: $\varkappa = 1,\ \lambda = 1$.

If the integral-equation is solved for a given contour $\vec{r}(s,y)$ and kinematic motion $\vec{v}_{kin}(s,y,t)$, equations (39) and (40) may be used to evaluate the resulting relative velocity field $\vec{v}_{rel}$ in the exterior of B, on B and inside, where its deviation from zero is an intrinsic measure for the accuracy of the solution. One can easily show that on B the relative velocity field is given by:

$$\vec{v}^{+}_{rel}(\vec{r},t) = +j_y \cdot \vec{t}_s - j_s \cdot \vec{t}_y \quad . \qquad (41)$$

The integral (24) has to be evaluated outside and inside of B for a given field point $\vec{r}$, and $\vec{v}_{kin}(\vec{r},t)$ subtracted according to equation (26).

The calculation of pressure, usually a most complicated venture for viscous fluids, may approximately be done by equation (6) in the limiting case of large Reynolds number. Combined with (24) we have on S:

$$\frac{1}{\rho_0} \int_{p_\infty}^{p^\pm} dp' = \frac{1}{2}\left(\vec{v}^{\pm}\right)^2 + \frac{d\Phi^\pm}{dt} \quad . \qquad (42)$$

If we subtract these two equations, the terms $(\vec{v}_+^{\,2} - \vec{v}_-^{\,2})$ cancel each other and (42) remains as:

$$\frac{1}{\rho_0} \int_{p^-}^{p^+} dp' = \frac{d}{dt}\left(\Phi^+ - \Phi^-\right) \quad . \qquad (43)$$

The relation (30) permits an interpretation which has not yet been mentioned. Ampere's theorem (e.g. [3], p. 54) states, that the function σ may be understood also as doublet distribution of a scalar potential function Φ, for which holds $\sigma = \Phi^+ - \Phi^-$.

Since $p^- = p_\infty$, the pressure coefficient is given by:

$$c_p = \frac{p^+ - p_\infty}{\frac{1}{2}\rho_0 u_\infty^2} = \frac{2}{u_\infty^2}\left\{\frac{\partial}{\partial t} + j_y \frac{\partial}{\partial s} - j_s \frac{\partial}{\partial y}\right\}\sigma(s,y,t) \quad . \tag{44}$$

The thin plate approximation yields the pressure difference between the upper and lower sides in the same way:

$$\Delta c_p = \frac{p^- - p^+}{\frac{1}{2}\rho_0 u_\infty^2} = -\frac{2}{u_\infty^2}\frac{d\sigma}{dt} = -\frac{2}{u_\infty^2}\left[i\omega + u_\infty \frac{\partial}{\partial x}\right]\sigma \quad . \tag{45}$$

The pressure coefficient for the steady case is given by:

$$c_p = 1 - \frac{\vec{v}_{rel}^{\,2}}{u_\infty^2} \quad . \tag{46}$$

This method is applied to Jukowsky-profiles of 12% thickness and at different angles of attack. The steady flow around a circular cylinder is computed; as the boundary condition, the potential flow condition $j_y = 0$ is taken. The results are in excellent agreement with the analytical solution. This substantiates the conjecture, that both boundary conditions for $\vec{\gamma}$ have their own importance.
Thin plate approximation is evaluated for steady and unsteady case and compared to analytical solutions for large aspect ratios. The formulas for the analytical solutions may be found e.g. in FOERSCHING [6] and SCHLICHTING & TRUCKENBRODT [7].
The necessary explanations may be found on the following pages.

5. Concluding Remarks

The method presented here is primarily designed to calculate the unsteady airloads of three-dimensional rotary wings in incompressible flow. The main objective of this paper has been to make the reader familiar with some basic considerations and properties of the approach. Therefore, applications are made to classical configurations, which allow comparisons to other methods and permit calculations of numerical errors. These classical solutions have been achieved by approximating step by step the VTE, which, even in the limiting case of very high Reynolds number, is a highly nonlinear integro-differential equation. This equation remains to be solved if the assumed approximations are no longer valid. In this case, the solution for the limiting cases considered here may be used as initial values for the iteration procedure.

To obtain a linear integral equation, the influence of vorticity on itself and the resulting relative velocities have to be omitted in the equation. One must keep this fact in mind, if one is talking about "exact" two-dimensional solutions for incompressible flow. The VTE seems to be the much more selfexplaining equation compared to the potential equation (7) for infinite

speed of sound. The duality of both formulations is very thoroughly discussed by MARTENSEN [8].
It is an important feature of the prensented approach, that the calculation of relative velocity for any solution inside the moving body or wing represents an intrinsic measure of accuracy at arbitrary points of the body. This property is no longer applicable when so-called source distributions are employed to produce thickness effects. For comparison of experimental data and and theoretical computations, it is worthwile to know, wether deviations between theoretical predictions and experimental results arise from inevitable numerical errors or are due to physical simplifications in the mathematical equations, which suppress certain properties of the real flow.
There is no doubt that incompressible flow is a very poor description of the fluids behaviour around helicopter blades. Nevertheless, it seems desirable to have reliable limiting cases of solutions, which also take compressibility into account.
In addition, there are certain applications (e.g. windmills), where incompressible flow is a good approximation for calculating airloads. In this application the inhomogenity of the onset flow causes the major part of mathematical problems compared to neglected compressibility effects.

REFERENCES

[1] PRAGER,W. Die Druckverteilung an Koerpern in ebener Potentialstroemung
Phys. Z. 29, 865 (1928)

[2] MARTENSEN,E. Berechnung der Druckverteilung an Gitterprofilen in ebener Potentialstroemung mit einer Fredholmschen Integralgleichung
Arch. Rat. Mech. Anal. 3, 235 (1959)

[3] MARTENSEN,E. Potentialtheorie, Stuttgart 1968

[4] LIGHTHILL,M.J. II. Introduction. Boundary Layer Theory
Laminar Boundary Layers, Oxford 1963
Editor: L. Rosenhead

[5] KRESS,J. Ueber die Integralgleichung des Praqerschen Problems
Arch. Rat. Mech. Anal. 30, 381 (1968)

[6] FOERSCHING,H.W. Grundlagen der Aeroelastik
Berlin/Heidelberg/New York 1974

[7] SCHLICHTING,H.& TRUCKENBRODT,E. Aerodynamik des Flugzeuges I
Berlin/Goettingen/Heidelberg 1959

[8] MARTENSEN,E. Die Dualitaet des Robinschen und Praqerschen Problems in drei Dimensionen
Arch. Rat. Mech. Anal. 30, 360 (1968)

[9] KRAEMER,K. Die Potentialstroemung mit Totwasser an einer geknickten Wand
Ingenieur-Archiv 33, 36 (1963)

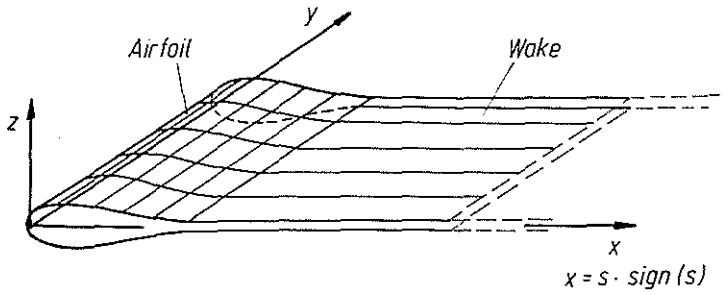

Fig. 1: Infinitely thin boundary layer

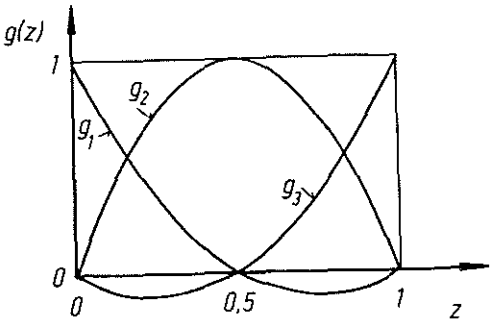

Fig. 3a: Functions q_l, Eq. (38)

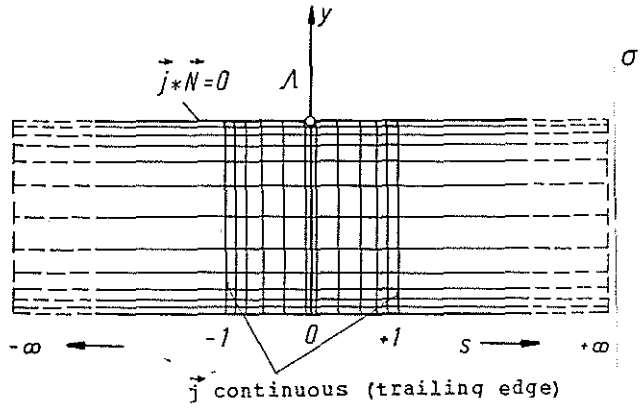

Fig. 2: Panel arrangement (Parameter domain)

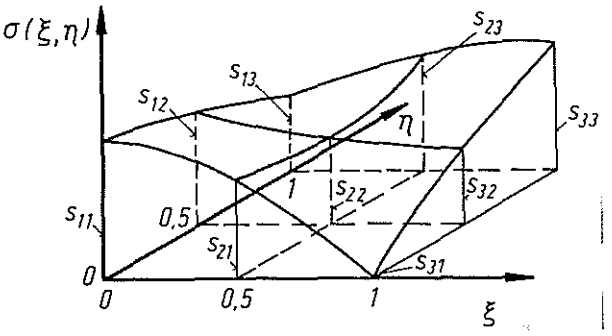

Fig. 3b: Function sigma, Eq. (36)

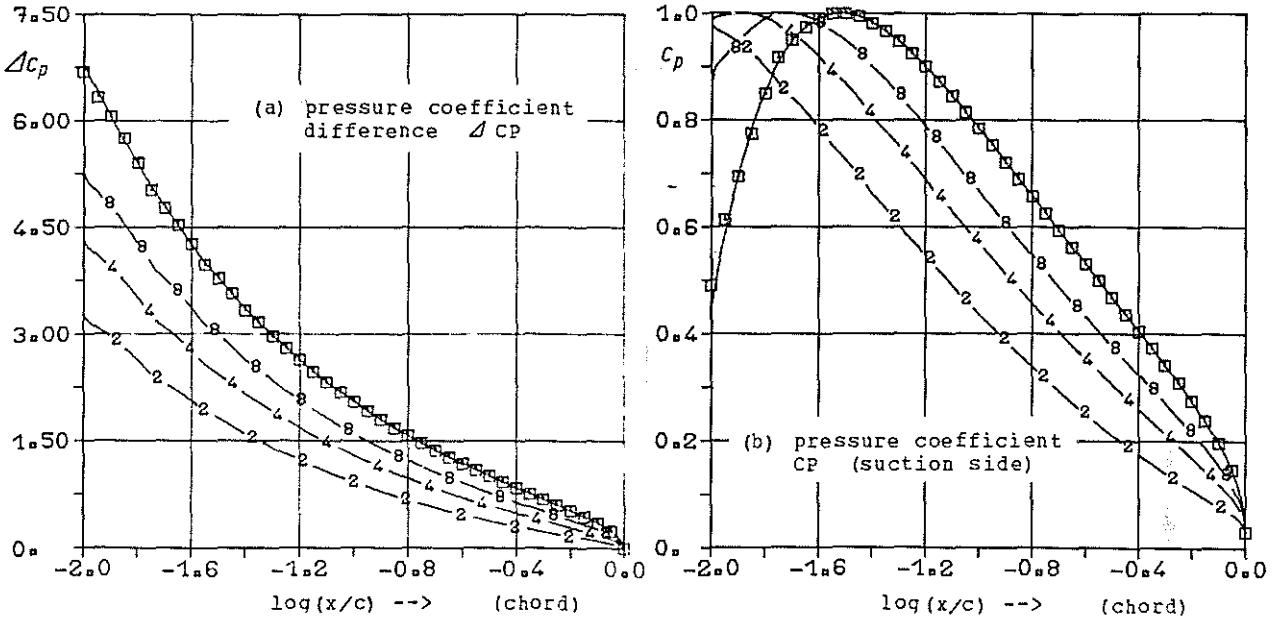

Fig. 4a and b: Thin plate approximation (steady flow)
Angle of attack: 10. degree
Aspect ratios (AR): 2, 4, 8 and 1000 (_□-□_)
Spanwise location: y/AR = 0.5
Analytical solution: ————

(a)

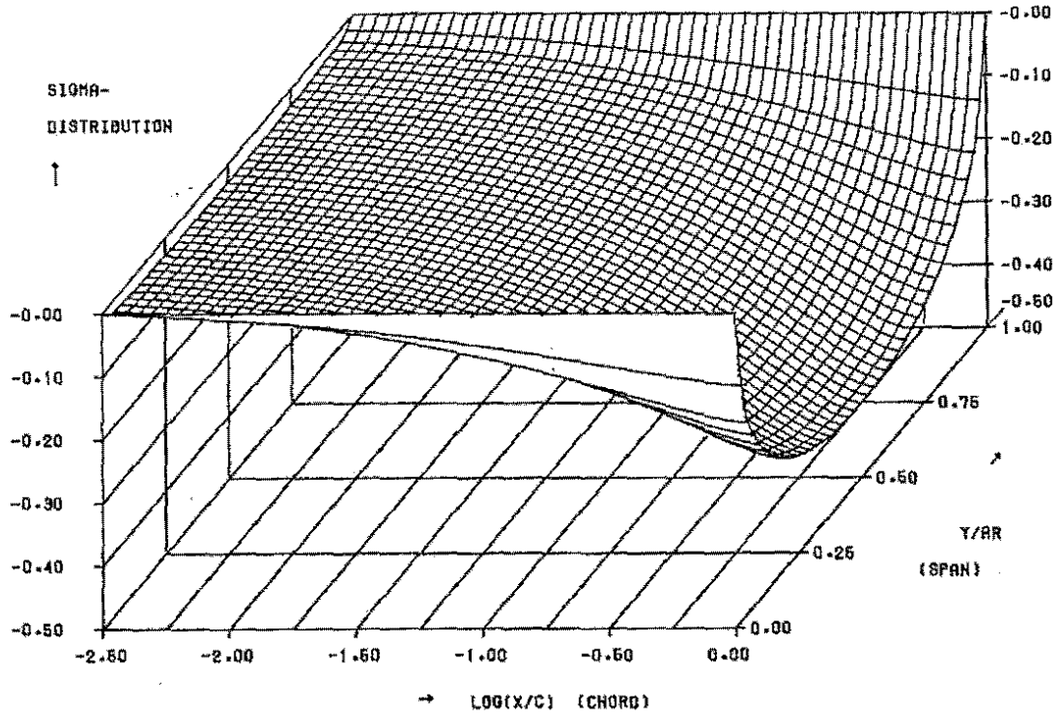

(b)

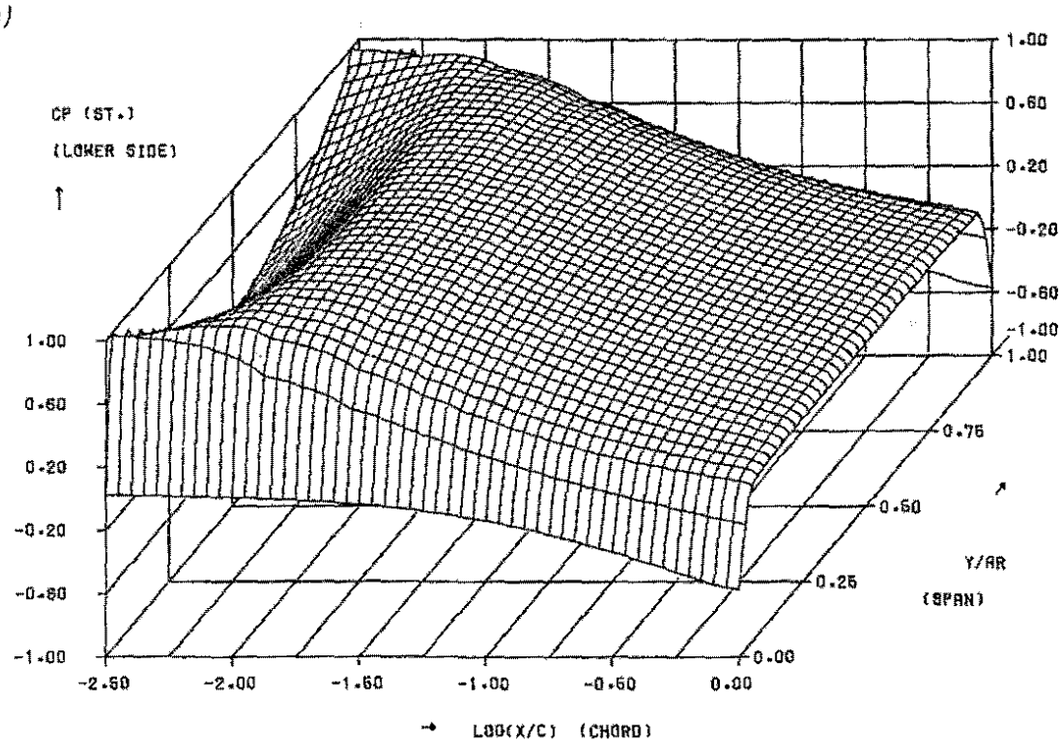

Fig. 5a and b: Thin plate approximation (steady flow)
Angle of attack: 10 deg., aspect ratio: 4.
(a) function sigma, (b) pressure coefficient
Log(x/c) = -2.5 <--> x/c ≅ 0.003

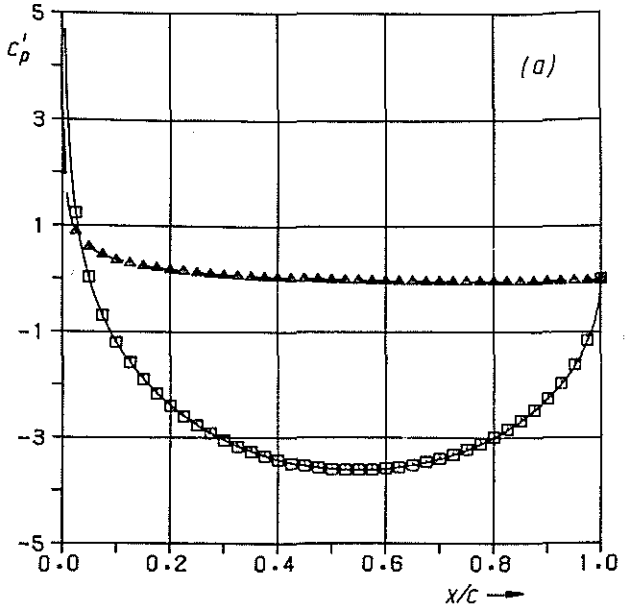

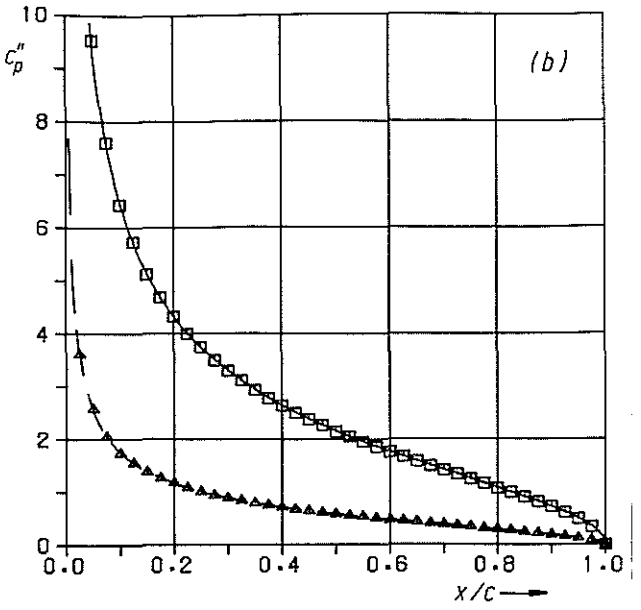

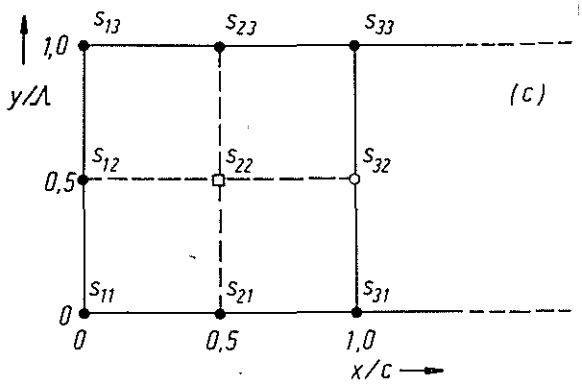

(a) and (b): 20 panels in chordwise direction

(c): plate approximated by one element

- Boundary condition Eq. (31)
- o $\vec{j}$ continuous
- Integral equation reduces to one single linear equation for S_{22}

(d) and (e): Computed solution for one element. (contains all basic features!)

Legend:

ω^*	computed	2-dim. sclution
0.2	△-△-△	— — —
1.0	□-□-□	—— ——

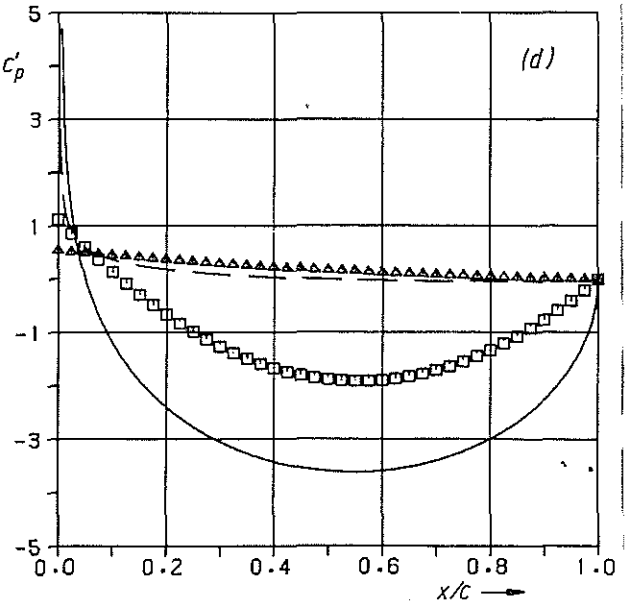

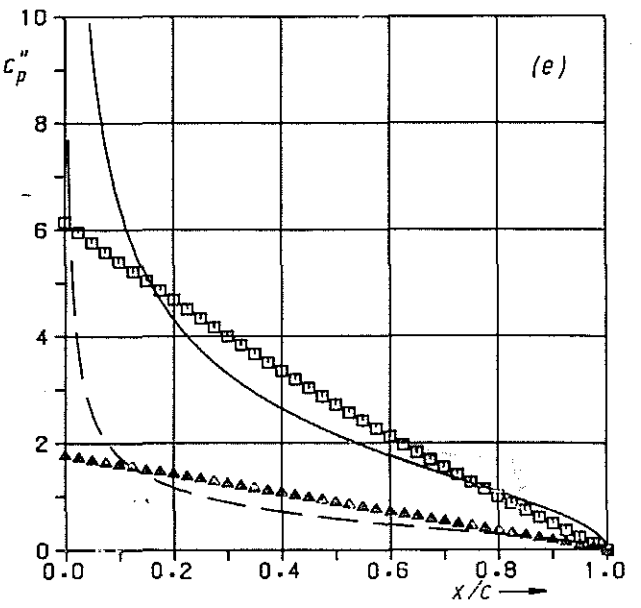

Fig. 6a - e: Thin plate approximation (unsteady flow)
Harmonic oscillation perpendicular to the onset flow
for two reduced frequencies ω^* (cf. [6], p. 257)
Angle of attack: 0 deg., aspect ratio: 1000.
Difference of complex pressure coefficient: $\Delta\overline{CP}$
$\Delta CP = CP' + i \cdot CP''$

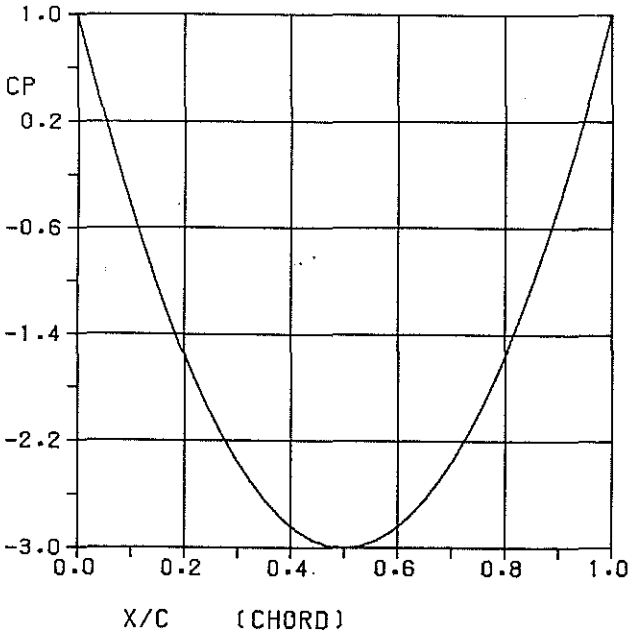

Fig. 7: Circular cylinder in steady flow pressure coefficient (symmetry plane)

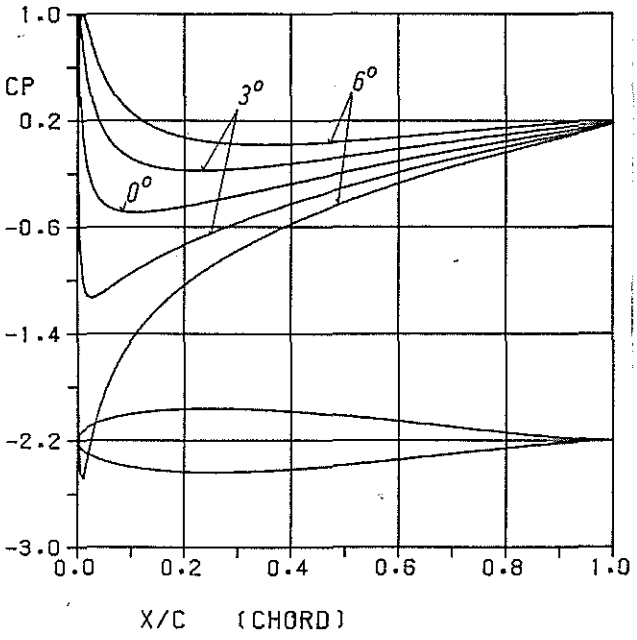

Fig. 8: Jukowsky profile in steady flow pressure coefficient (symmetry plane) Angles of attack: 0., 3. and 6. degree

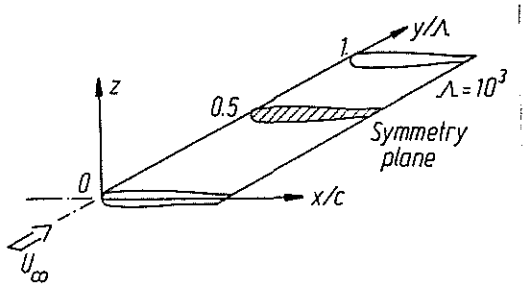

Fig. 9: Geometry

Circular Cylinder

Angle of attack: 0. degree
CP(2D): Analytical solution
CP(3D): Computed solution
Aspect ratio 3D: 1000.

X	CP(2D)	CP(3D)	2D-3D	ERROR %
0.0	1.0000	1.0000	0.00000	0.000
0.0100	0.8416	0.8427	-0.00115	-0.137
0.0200	0.6864	0.6891	-0.00271	-0.395
0.0300	0.5344	0.5369	-0.00252	-0.471
0.0400	0.3856	0.3860	-0.00045	-0.117
0.0500	0.2400	0.2432	-0.00324	-1.349
0.1000	-0.4400	-0.4371	-0.00293	0.666
0.1500	-1.0400	-1.0371	-0.00287	0.276
0.2000	-1.5600	-1.5563	-0.00375	0.240
0.2500	-2.0000	-1.9965	-0.00353	0.177
0.3000	-2.3600	-2.3577	-0.00234	0.099
0.3500	-2.6400	-2.6387	-0.00132	0.050
0.4000	-2.8400	-2.8363	-0.00369	0.130
0.4500	-2.9600	-2.9564	-0.00357	0.121
0.5000	-3.0000	-2.9996	-0.00039	0.013

Tab. 1: Comparison of computed solution and analytical solution

Jukowsky Profile 12 %

Angle of attack: 0. degree
CP(2D): Analytical solution
CP(3D): Computed solution
Aspect ratio 3D: 1000.

X	CP(2D)	CP(3D)	2D-3D	ERROR %
0.0	1.0000	1.0000	-0.00000	-0.000
0.0100	0.0886	0.0926	-0.00402	-4.543
0.0200	-0.1862	-0.1796	-0.00664	3.568
0.0300	-0.3139	-0.3099	-0.00396	1.261
0.0400	-0.3844	-0.3840	-0.00038	0.099
0.0500	-0.4270	-0.4236	-0.00337	0.790
0.1000	-0.4899	-0.4885	-0.00139	0.283
0.1500	-0.4772	-0.4764	-0.00084	0.176
0.2000	-0.4445	-0.4439	-0.00066	0.149
0.2500	-0.4045	-0.4040	-0.00049	0.120
0.3000	-0.3614	-0.3611	-0.00036	0.098
0.3500	-0.3174	-0.3171	-0.00028	0.089
0.4000	-0.2734	-0.2731	-0.00024	0.089
0.4500	-0.2298	-0.2296	-0.00020	0.086
0.5000	-0.1871	-0.1869	-0.00018	0.096
0.5500	-0.1454	-0.1452	-0.00015	0.105
0.6000	-0.1048	-0.1046	-0.00015	0.140
0.6500	-0.0653	-0.0652	-0.00017	0.259
0.7000	-0.0271	-0.0269	-0.00019	0.694
0.7500	0.0099	0.0101	-0.00023	-2.309
0.8000	0.0456	0.0459	-0.00030	-0.658
0.8500	0.0801	0.0806	-0.00041	-0.510
0.9000	0.1135	0.1140	-0.00051	-0.450
0.9500	0.1456	0.1459	-0.00031	-0.211
0.9600	0.1519	0.1521	-0.00016	-0.109
0.9700	0.1581	0.1581	0.00006	0.036
0.9800	0.1643	0.1640	0.00030	0.184
0.9900	0.1705	0.1700	0.00043	0.251
1.0000	0.1766	0.1803	-0.00371	-2.102

Tab. 2: Comparison of computed solution and analytical solution

Jukowsky profile 12%

Angle of attack: 0. degree
Aspect ratio(AR): 8.
Panel elements: 30 chordwise direction
(15 for each side)
7 spanwise direction

Relative velocity VREL inside and outside the profile along selected directions. The approximation of the profile by a cylindrical surface causes the error in CP (pressure coeff.) for Y/AR -> 1.

1. Chordwise direction along x (symmetry plane)

X/C	Y/AR	Z	CP	VREL.X	VREL.Y	VREL.Z
-0.1000	0.5000	0.0	0.2408	0.8713	-0.0000	0.0000
-0.0500	0.5000	0.0	0.4000	0.7746	-0.0000	0.0000
0.0500	0.5000	0.0	0.9999	0.0082	0.0000	0.0000
0.1000	0.5000	0.0	1.0000	0.0035	0.0000	0.0000
0.2000	0.5000	0.0	1.0000	0.0013	0.0000	0.0000
0.4000	0.5000	0.0	1.0000	0.0003	0.0000	0.0000
0.6000	0.5000	0.0	1.0000	0.0003	0.0000	0.0000
0.8000	0.5000	0.0	1.0000	0.0011	0.0000	-0.0000
0.9000	0.5000	0.0	1.0000	-0.0031	0.0000	-0.0000
0.9500	0.5000	0.0	0.9999	-0.0084	0.0000	0.0000
0.9900	0.5000	0.0	1.0000	-0.0015	0.0000	-0.0000
0.9990	0.5000	0.0	1.0000	-0.0024	0.0000	-0.0000
0.9999	0.5000	0.0	0.9998	-0.0156	0.0000	0.0000

2. Vertical direction (inside and outside)

X/C	Y/AR	Z	CP	VREL.X	VREL.Y	VREL.Z
0.2500	0.5000	0.0	1.0000	0.0012	0.0000	0.0000
0.2500	0.5000	0.010000	1.0000	0.0013	0.0000	-0.0002
0.2500	0.5000	0.020000	1.0000	0.0015	0.0000	-0.0004
0.2500	0.5000	0.040000	1.0000	0.0029	0.0000	-0.0021
0.2500	0.5000	0.050000	1.0000	0.0047	0.0000	-0.0052
0.2500	0.5000	0.059000	0.9998	0.0054	0.0000	-0.0125
0.2500	0.5000	0.059744	0.9998	0.0052	0.0000	-0.0133
0.2500	0.5000	0.059745	-0.4118	1.1881	-0.0000	0.0179
0.2500	0.5000	0.060000	-0.4116	1.1880	-0.0000	0.0177
0.2500	0.5000	0.080000	-0.3708	1.1707	-0.0000	0.0121
0.2500	0.5000	0.100000	-0.3347	1.1552	-0.0000	0.0148
0.2500	0.5000	0.500000	-0.0693	1.0340	-0.0000	0.0090
0.2500	0.5000	1.000000	-0.0219	1.0109	-0.0000	0.0021
0.2500	0.5000	2.000000	-0.0055	1.0028	-0.0000	0.0003
0.2500	0.5000	5.000000	-0.0006	1.0003	-0.0000	0.0000

3. Spanwise direction

X/C	Y/AR	Z	CP	VREL.X	VREL.Y	VREL.Z
0.5000	0.5000	0.0	1.0000	0.0002	0.0000	-0.0000
0.5000	0.6000	0.0	1.0000	0.0022	0.0048	-0.0000
0.5000	0.7000	0.0	0.9999	-0.0008	0.0081	-0.0000
0.5000	0.8000	0.0	0.9995	-0.0200	0.0119	-0.0000
0.5000	0.9000	0.0	0.9952	0.0595	0.0357	0.0000
0.5000	0.9500	0.0	0.9474	0.2068	0.0989	-0.0000
0.5000	1.0000	0.0	0.1021	0.9242	0.2091	0.0000

****
****